Published as:

Blank, M., & Weber, L., Towards a coherent database of thermal boundary conductance at metal/dielectric interfaces. *Journal of Applied Physics*, *125*(9) (2019) 095302, DOI: 10.1063/1.5085176

ABSTRACT

The Thermal Boundary Conductance (TBC) of metal/dielectric couples was measured for a large variety of metals on silicon, sapphire and diamond using Time Domain Thermoreflectance and compared to data previously obtained on diamond. In the case of silicon, HF-cleaned and RF-etched surfaces were tested. The detailed structure of these interfaces was studied, allowing distinction of two different cases of M/Si couples: i) some amount of interfacial reaction exists for both surface terminations, resulting in similar TBCs; and ii) chemically abrupt interfaces are achieved, resulting in TBC values that are always lower for RF-etched samples. The TBC values obtained on different substrates allowed identifying a tendency of the TBC to scale with the Maximum Transmission Limit (MTL). A possible influence of the substrate was evaluated using both the Diffuse Mismatch Model (DMM), which predicts a strong dependence on the substrate properties and a newly developed approach based on the metal irradiance (IM), which predicts no dependence on the substrate properties. The DMM was implemented using a Debye model with either a linear (DMM_{Linear}) or a Sine-Type ($DMM_{SineType}$) dispersion, while the IM was implemented using a Sine-Type ($IM_{SineType}$) dispersion. The DMM_{Linear} and the $IM_{SineType}$ were found to be more suitable than the $DMM_{SineType}$ and to be equally precise in predicting TBC at metal/silicon and metal/sapphire interfaces. The $IM_{SineType}$ is found to be better suited than both the DMM_{Linear} and the $DMM_{SineType}$ to predict TBC at metal/diamond interfaces. $IM_{SineType}$ being the only model tested that is suitable for all three substrates, it appears to be the most appropriate choice. As a corollary we find that the TBC dependence on substrate properties is much weaker than predicted by the DMM.

I. INTRODUCTION

Downsizing of devices to the nanoscale raises several new scientific challenges. Amongst others, interfacial properties are of prime importance because they strongly influence the overall efficiency in many applications. In the field of thermal management, for example, resistance to heat flow at interfaces often exceeds the one in the small-scaled bulk forming the interface. This is particularly true at metal-dielectric interfaces in which the Kapitza length, i.e. the equivalent thickness of bulk material forming the same resistance to heat flow as the interface, at ambient can be as large as 200 µm (e.g. at Bi/H:diam interface (1)). A variety of studies investigated the mechanisms involved in such systems. Experimentally, the effect of material mismatch (1,2), bond strength (3–5) and interfacial roughness (6–9) on TBC were extensively explored. In parallel, significant efforts were dedicated to developping a model that accurately predicts the TBC. The Diffuse Mismatch Model (DMM) (10) is the most widely used for metal/dielectric couples at room temperature. It relies on the importance of a change in acoustic properties with two general tendencies: i) the TBC decreases with increasing mismatch in phonon density of states (p-DOS) on either side of the interface and ii) the TBC is strongly sensitive to the substrate properties. The simplest form of the DMM uses the Debye model with a linear dispersion relation. A further restriction of the DMM is that it takes only elastic processes into account. These simplifications result in limited agreement between experimental and theoretical values. Many adaptations were explored to refine the predictions. Amongst others, more realistic phonon dispersions relations were used (11), while modified models were proposed that take into account additional interfacial states (12) or possible inelastic interactions (13), for example. None of these were, however, able to capture the full picture of the physics involved but all of them kept the general trend described above. More recently, Monachon *et al.* (14) suggested that metal irradiance instead of p-DOS mismatch might be a suitable parameter to predict thermal transport at metal/dielectric interfaces. This approach entails that, unlike predicted by the DMM, the substrate has no influence on the TBC. Instead, solely the phonons in the metal have to be taken into account. The validity of this model was discussed

based on a number of values obtained both from authors' earlier works and from the literature.

The endeavour to validate models by experimental data is rendered difficult by the fact that the specific setups, preparation techniques, characterization techniques, and data extraction models vary significantly amongst the contributing groups, blurring the big picture and trends in TBC. In the present study we provide systematic measurements of TBC of a wide range of metals on some of the most popular substrates, i.e. silicon, sapphire, and diamond, using identical sample preparation, characterization methods, and data analysis. The thus generated TBC values are complemented by measurements previously performed on diamond (15), obtained on a very similar setup, and are meant to serve as a database that allows for a comprehensive comparison of experimental data to predictive models. It is believed that analysing such a large number of data, coming from one single source, is a promising way to deepen our understanding about the mechanisms that are involved in thermal transport at metal/dielectric interfaces and their relative importance. Since metal and silicon are likely to react together and to form some interfacial compounds, a detailed exploration of metal/silicon is further conducted for two different sample preparation techniques. This complementary information is believed to provide a way to avoid bias related to uncontrolled interfacial properties.

II. EXPERIMENTAL METHOD

a. Sample preparation and characterization

An Alliance-Concept DP 650 sputtering machine was used to deposit a wide variety of metals (Ag, Al, Au, Cr, Cu, Ir, Mo, Ni, Pd, Pt, Ta, Ti and W) on silicon and on sapphire and (Ag, Au, Cu, Ir, Ni, Pd, and Ta) on diamond. A thin Cr cover-layer was further added on top of each sample to act as a transducer, i.e. a cap layer with high change in reflectance with temperature. The samples were kept under vacuum during the whole stack deposition process.

525 µm-thick, boron-doped [100] Si wafers were used for all metal/silicon samples. Their surface state was imposed by an RCA cleaning step. Right before

deposition, each wafer was further dipped into a 10%-HF solution during 1 min, providing an oxide-free, H-terminated surface (16). This surface state could then be changed into a Si-terminated surface by performing a 60s RF-etch (16) within the DP650 sputtering machine. These two different surfaces are referred as "HF-dipped" (HF) and "RF-etched" (RF) respectively. Ag, Au, Cu, Cr, Mo, Ni, Pd, Pt and Ta were deposited on both HF and RF surfaces.

600 μm-thick c-plane [0001] Al_2O_3 wafers purchased from UniversityWafer (Ref. 2561) were used for all metal/sapphire samples. Each wafer was cut into 2x1cm^2 pieces using a Disco DAD321 dicing saw before being ultrasonically cleaned successively in acetone, ethanol and isopropanol. Possible organic contamination was removed with a 2 min Ar:O plasma treatment using a Fischione 1020 with a 3:1 Ar:O_2 gas mixture.

1 mm-thick [001] HPHT diamond stones purchased at Element 6 (Shannon, Co. Clare, Ireland, Ref: MWS L25) were mechanically polished using successively 6, 3 and 1 μm diamond paste with olive oil as a lubricant. Fine polishing was performed using 1 μm diamond paste and a mixture of soap, ethanol and water as a lubricant. Surface reactivity was induced with a 15 min Ar:O-plasma treatment similar to the one described above.

The thickness of each layer was measured by X-Ray reflectivity (XRR) using a XRD Empyrean Diffractometer. Fitting of the curves was obtained with the GenX software (17). Fitting parameters were i) the thickness, ii) the density and iii) the roughness of the layers and substrate and iv) the width of a possible intermixed zone between two neighbouring layers.

In the case of metal/silicon samples, a set of verification samples were analysed by TEM. All samples were mechanically polished and ion milled until electron transparency was achieved. Ion milling temperature and beam power were set to -100°C and 0.2 keV, thus avoiding any structural change of the interface due to sample heating. All samples were observed using a FEI-Tecnai Osiris microscope operating at 200 kV.

b. Thermal boundary conductance measurement

The Time Domain Thermo-Reflectance (TDTR) technique was used to measure the thermal boundary conductance at metal/dielectric interfaces. The setup used in this work is similar to the one described previously (15,18). In a nutshell, the laser source was a COHERENT Mira 900 with a repetition rate of 76 MHz and an operation wavelength of 785 nm. The initial beam was separated into a pump and a probe. The pump was modulated at 10.7 MHz using an Electro-Optic Modulator (EOM) before both beams were focused on the sample surface. There, the pump heats the sample surface, while the probe monitors the temperature change through a variation of sample reflectivity. The signal obtained was collected using a fast photodiode (Thorlabs GmbH, Ref: DET10A), before being frequency filtered at the pump modulation frequency, pre-amplified and fed into a ZI-HF2 digital lock-in amplifier (Zurich Instruments, Zurich, Switzerland). Full cooling curves were obtained using a delay stage that was inserted on the pump optical path and that allowed sweeping delay times ranging from 0 to 4 ns. A good signal-to-noise ratio was ensured by differentiating the pump and the probe polarizations and wavelengths using a so-called “two-tint” technique (18), which minimizes the noise coming from the pump.

A power meter and a CMOS camera were used to measure the exact fluence and $1/e^2$ radius of each experiment with target values being 0.2 mJ/m^2 and 4 µm, respectively.

Experimental curves were analysed by fitting the X/Y ratio extracted from the lock-in signal to the model proposed by Cahill (19). TBC and substrate conductivity were used as fitting parameters, while the thermal conductivity and heat capacity of the metallic layers as well as the substrate’s heat capacity were taken from the literature (20). The metallic layer thicknesses were taken from XRR measurements, as described above. The exact same procedure was used for the intermixed region at metal/Si interfaces (cf. Section IV.b). As shown in Fig. 1, a good signal-to-noise ratio as well as a good fit quality were obtained for all metals on all substrates.

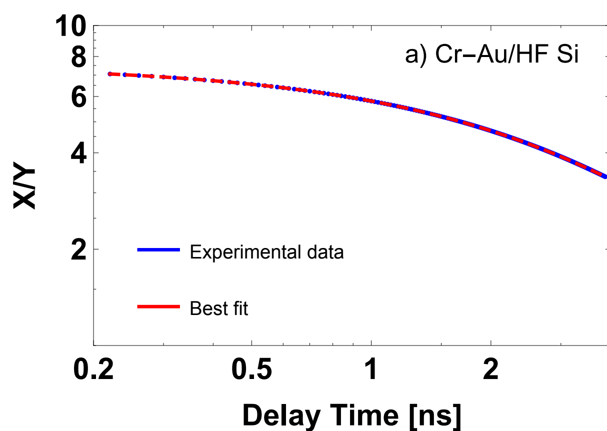

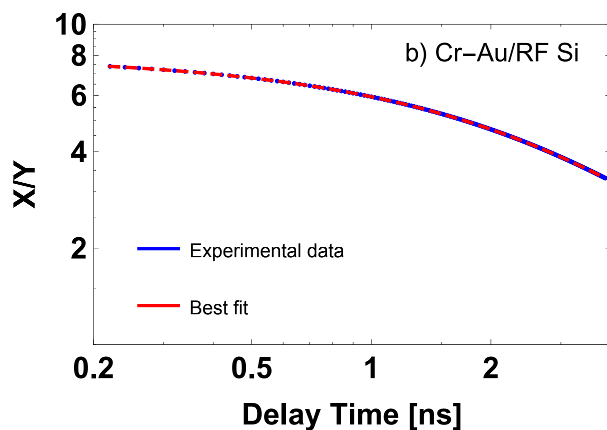

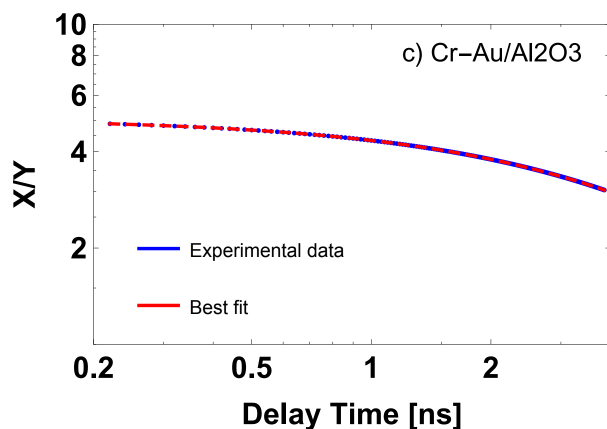

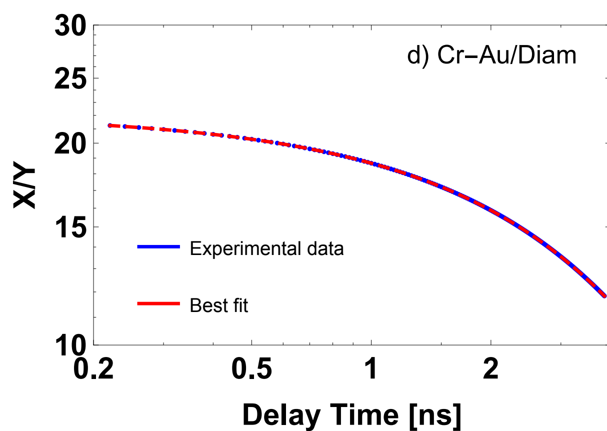

Figure 1: TDTR raw signals and fitting curves obtained for a) Cr-Au/HF Si b) Cr-Au/RF Si c) Cr-Au/sapphire and d) Cr-Au/diam.

III. RESULT

a. XRR as a characterization tool to explore the detailed structure of metal/silicon interfaces

XRR was found to be a suitable technique to detect the existence of possible intermixed regions at metal/Si interfaces with thicknesses ranging from 0.1 to 10 nm. In cases where such a layer existed, ignoring it would prevent proper data fitting, as shown in Fig. 2a. Instead, assuming the presence of a layer that has a 50:50 compositional ratio led to satisfactory fits (Fig. 2b.). The presence of such intermixed layers was verified by performing TEM imaging on a set of control samples. Comparing the results obtained using both techniques, it is observed that the XRR is well suited to detect the existence of an intermixed layer. However, the lack of information on the detailed composition of this region led to considerable uncertainty in quantitative assessment its thickness. As shown in Table 1, assuming a 50:50 compositional ratio can lead to thickness measurements errors larger than a factor of 2.

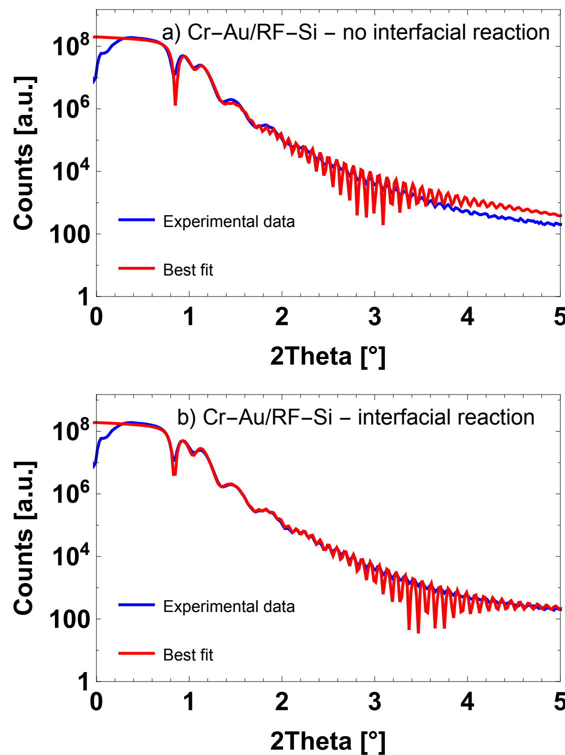

Figure 2: X-Ray Reflectivity (XRR) experimental data and fitting curves for Cr-Au/RF-etched Si with a) fitting performed without taking into account a possible interfacial reaction between Au and Si, b) fitting performed taking into account a possible interfacial reaction between Au and Si

Table 1: Comparison between the intermixed region thicknesses measured using both the XRR and TEM imaging. The XRR measurement strongly depends on the intermixed region composition, which is unknown. This results in relatively large errors in the values found for intermixed region thicknesses.

Couple	XRR interlayer thickness HF-dipped [nm]	TEM interlayer thickness HF-dipped [nm]	XRR interlayer thickness RF-etched [nm]	TEM interlayer thickness RF-etched [nm]
Ag/Si	2.1		1.6	
Al/Si	-		-	
Au/Si	2.2	~1.5	5	~3.8
Cr/Si	-		-	
Cu/Si	-	-	-	disordered silicon
Ir/Si	1.4		N.A.	
Mo/Si	-		-	
Ni/Si	2.5		2.6	
Pd/Si	2.1		5.4	
Pt/Si	4.6	~6.5	4.3	~10
Ta/Si	2		2.2	
W/Si	2.6		N.A.	

b. Detailed structure of metal/silicon interfaces and its influence on TBC

As shown in Fig. 3, the exploration of the detailed structure of metal/silicon interfaces allowed distinction of two cases: i) flat interfaces with some intermixing formed for both metal/HF-dipped Si and metal/RF-etched Si samples, as e.g. for Au, Ag, Pd, Pt, Ni and Ta/Si interfaces; ii) chemically abrupt interfaces with no intermixing, found in Al, Cr, Cu and Mo/Si couples. In the latter case, metal/HF-dipped interfaces are observed to be flat, while some amount of structural disorder is observed at the metal/RF-etched Si interface.

Fig. 4 shows the results obtained for these various interfaces as a function of the Maximum Transmission Limit (MTL) of each metal. The MTL was chosen because it gives the highest physically possible TBC, assuming that all phonons coming from the metal are transmitted to the dielectric either via harmonic or anharmonic interactions. This allows analysing TBC values by preventing any possible influence coming from the assumptions made in commonly used models such as AMM, DMM, RL, etc. The typical experimental variability of a set of

measurements performed on the same sample was found to be smaller than 7%, while the overall precision is evaluated to be ±20% and takes into account the uncertainty on the layer thicknesses and thermal properties, on the laser spot size and on the beam power.

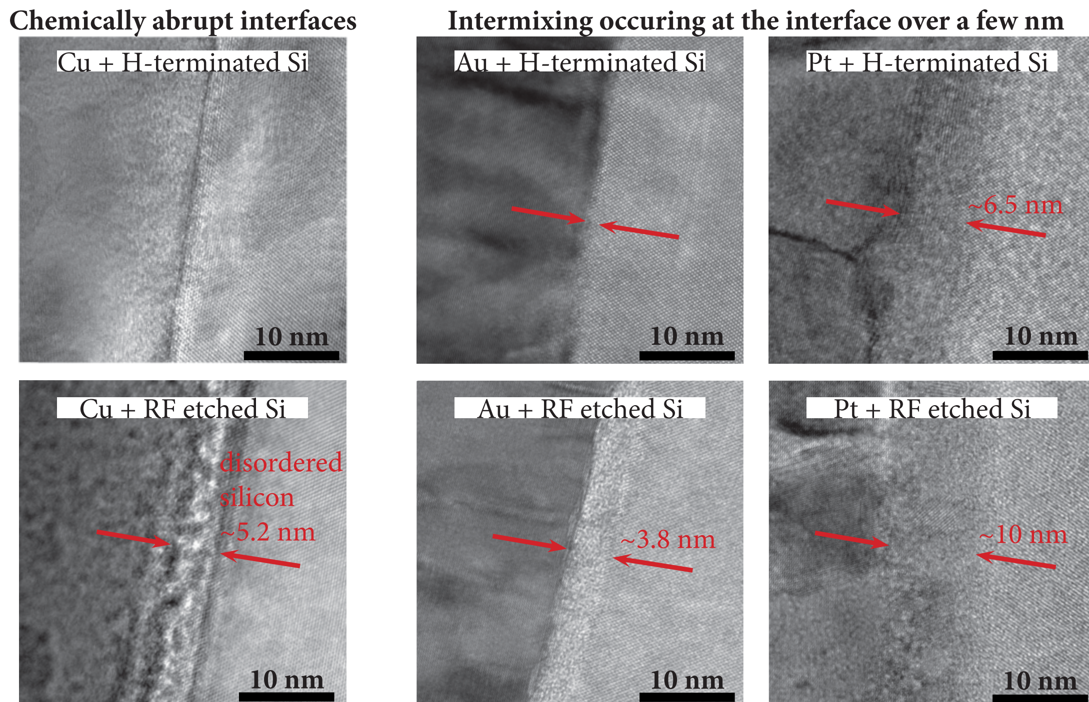

Figure 3: TEM images performed on a set of control samples, confirming that XRR is a suitable method to determine whether intermixing occurred at metal/silicon interfaces.

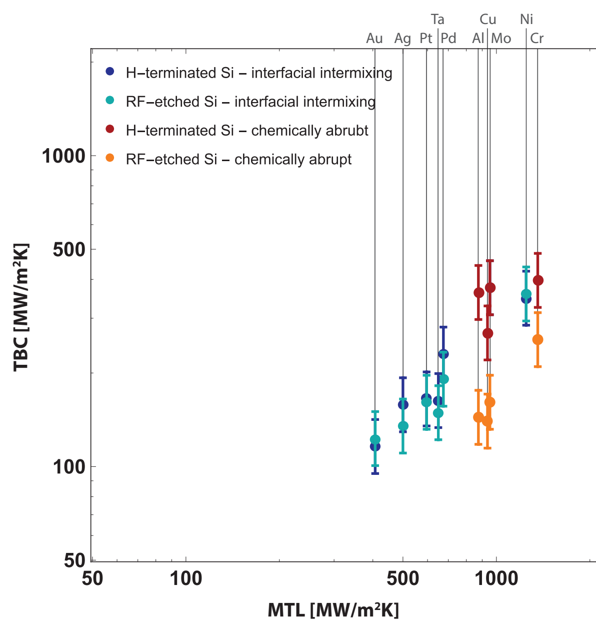

Figure 4: TBC measured at metal/silicon interface with HF-dipped and RF-etched silicon surface.

Depending on whether the metal/Si interface studied is according to the first or the second case, the TBC is seen to evolve differently. On the one hand, it is observed that for all metal/Si interfaces in which interfacial intermixing was present, the TBC does not depend on the silicon surface preparation technique prior to deposition. On the other hand, for all metals that exhibited a chemically abrupt interface, TBC was observed to be larger for HF-dipped substrates than for RF-etched substrates, with the TBC of the HF-dipped sample being typically 1.5 to 2.5 times larger than the TBC of the RF-etched sample.

c. TBC dependence on substrate

Fig. 5 summarizes the results obtained for TBCs measured for a variety of metals on silicon, sapphire and diamond as a function of the MTL. As for the values presented in Section III.a, the typical experimental variability of a set of measurements performed on the same sample was found to be smaller than 7%, while the overall precision is evaluated to ±20%. TBC values ranged roughly from 50 to 500 MW/m^{2}K (specific numerical values can be found in Supplemental Material Table 2). We further added in Fig. 5 the data measured by our group on diamond reported previously (15), as well as values found elsewhere in the literature for metal/silicon (21,22), metal/sapphire (2,21,23–25) and metal/diamond (26) couples. Our data are found to be overall in good agreement with values from the literature.

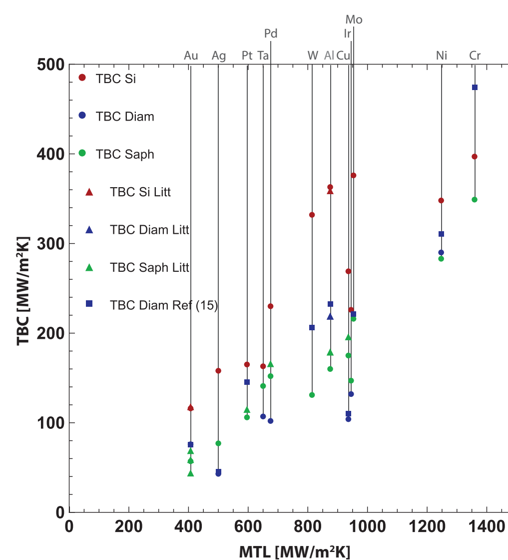

Figure 5: Compilation of TBC values measured at metal/silicon, metal/sapphire and metal/diamond interfaces. Dots are for measurements performed within this work (silicon and sapphire) or taken from (15) (diamond) and triangles are values taken from the literature (2,21–26).

For all substrates, TBC clearly tends to increase with increasing MTL. Au and Cr, which have respectively the lowest and the highest MTL amongst the metals tested (407 vs. 1359 MW/m^2K), accordingly exhibit the smallest and the largest TBC values with TBC at Cr interfaces being larger by a factor of 3.5 for silicon and by a factor of 6 for both sapphire and diamond substrates.

No clear trend in the influence of the substrate on the TBC could be identified. As an example, the TBC at Au, Al, Cr, Pt and W interfaces was found to be the lowest when using a sapphire substrate, while a diamond substrate was observed to lead to the smallest TBC at Ag, Cu, Ir, Pd and Ta interfaces.

IV. DISCUSSION

a. Occurrence of an intermixed region at metal/Si interface

Intermixing was observed at all metal/Si interfaces except for Al, Cu, Cr and Mo/Si interfaces. Interestingly enough, equilibrium phase diagrams indicate that Cu, Mo and Cr would be favourable to form silicides, while at thermodynamic equilibrium Ag, Au and Al would not be expected to form silicides. Seemingly, the sputtering conditions used within this work do not reflect equilibrium. Out-of-equilibrium compounds are formed instead, whose properties are not known. The existence of such non-equilibrium compounds for the Au/Si and Ag/Si systems have been observed by Klement and co-workers (27,28) at high cooling rates from the liquid. As will be detailed below, the combination of XRR measurements and TEM investigation still allowed extracting TBC values for those interfaces despite the lack of precise thermophysical properties of those interphases.

b. TDTR measurement sensitivity to an intermixed region

XRR measurements highlighted the existence of an intermixed region in many metal/Si couples. However, neither the exact composition, nor the exact thickness of these layers is known, preventing precise determination of their thermal properties. Compounds with various metal:Si ratio are however most likely formed. Based on literature values for silicides, they are expected to have a

thermal conductivity of about 20 W/mK and a volumetric heat capacity on the same order as the pure metal (29–31).

Taking these considerations into account, TBC values were extracted from TDTR curves with the intermixed region thermal properties being approximated as follows: i) its thermal conductivity was set to 20 W/mK, ii) its volumetric heat capacity was assumed to be the same than its metal counterpart and iii) its thickness was set based on the values obtained by XRR. While these approximations are fairly rough, i.e. the uncertainty in thickness can easily reach a factor of 2, cf. section III.2, and the uncertainty in heat capacity and thermal conductivity might be of the same order, a detailed analysis of TDTR sensitivity to the intermixed layer thermal properties was carried out. The sensitivity S to a parameter *i* is expressed using Eq. 1.

$$S_i(T) = \frac{\partial \ln\left[-\frac{X(t,T)}{Y(t,T)}\right]}{\partial \ln[i(T)]} \qquad (1)$$

The sensitivity to parameter *i* is low for *S* values close to zero and it scales with increasing *S* values. A low sensitivity to parameter *i* means that large errors in its determination will not significantly affect the end result. Similarly, a large sensitivity to parameter *i* means that even small errors in its determination can significantly affect the end result.

In the case of metal/Si couples, it was highlighted that none of the intermixed region thermal properties were critical in determining the final TBC value. As shown in Fig. 6: *S* values fall close to zero for all three parameters in all the systems studied and for all delay times. Consequently, errors due to rough approximations for the intermixed region thermal properties do not affect the final TBC values significantly.

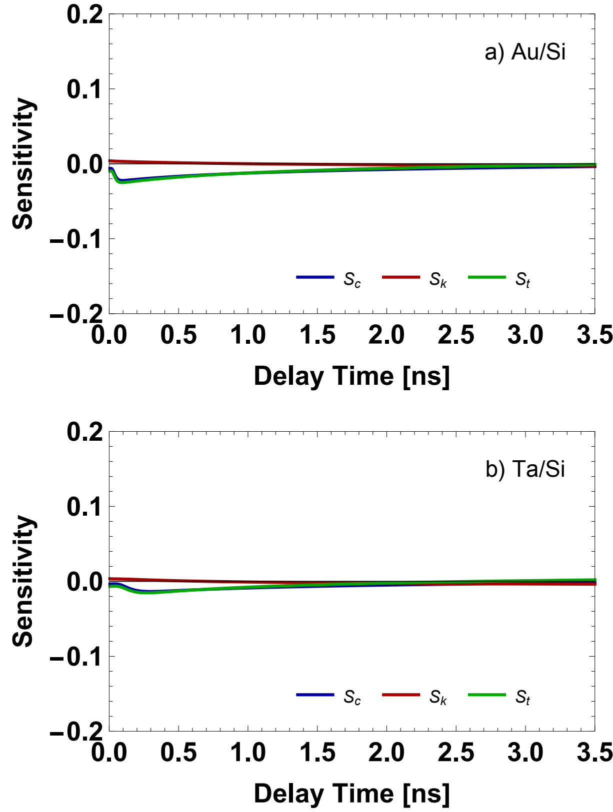

Figure 6: TDTR measurements' sensitivity to the intermixed region thermal properties.

c. Detailed structure of metal/silicon interfaces and its influence on TBC

The dependence of the TBC on the detailed structure of the metal/Si interface observed in Fig. 4 is rationalized as follows.

When an intermixed region exists for both the HF-dipped and the RF-etched samples, the metal/Si interfaces structure does not depend much on the surface preparation technique, except for the thickness that was shown to change by a factor that can be as large as 1.5 (e.g. Pt/Si, see Fig. 3). A possible change in composition cannot be excluded either. None of these parameters was however found to be critical enough to influence the TBC, resulting in values that are equal, within experimental errors, whatever surface termination is used. The same kind of behaviour was already observed at metal/diamond interfaces (32), in which TBC was observed to be the same for as-deposited samples and after a heat-treatment that enabled carbide formation. This was taken as a sign that interfacial carbides-like bonds controlling the TBC already exist in the as-

deposited sample. Similarly, the results obtained at Au, Ag, Pd, Pt, Nb and Ni/Si suggest that the nature of interfacial bonds that controls the TBC is the same in both cases.

When a chemically abrupt interface is obtained, the metal/Si interface structure depends significantly on the surface preparation technique. HF-dipped samples exhibit flat interfaces, while RF-etched samples display a much rougher interface in which some amount of disordered silicon is found to be present, most likely induced by the Ar-ion bombardment. These differences result in TBC values that are always lower for RF-etched samples with a relative decrease that ranges from a factor of 1.5 in the Cr/Si system to a factor of 2.5 in the Al/Si system. TBC reductions related to disordered interfaces were already observed (6,9) and attributed to a reduction in the phonon transmission probability, which comes from an increase in phonons scattering. Based on these observations, HF-dipped samples were used as a reference for the comparison with TBC measured on other substrates.

b. TBC dependence on substrate

In an attempt to deepen our understanding on the role of the substrate on TBC at metal/dielectric interfaces, TBC values obtained within this work combined with those previously obtained by our group on diamond (15) were compared to two different models proposed in the literature. On the one hand, the well-known DMM, which predicts a strong dependence of TBC on the relative phonon DOS on either side of the interface. This model was implemented using a Debye model with either a linear (DMM_{Linear}) (Eq. 2) or a Sine-Type ($DMM_{SineType}$) (33) (Eq. 3) dispersion relation.

$$\omega_{linear} = cK \quad \rightarrow \quad D_{linear}(\omega) = \frac{L^3 \omega^2}{2\pi^2 c^3} \qquad (2)$$

with ω the angular frequency, c the sound velocity and K the wave vector.

$$\omega_{SineType} = \omega_0 \sin\left(\frac{\pi}{2}\frac{K}{K_D}\right)$$

$$\rightarrow \quad D_{SineType}(\omega) = \int_0^{\omega_D} \frac{1}{\pi^2} N^{\frac{1}{3}} \left(\frac{6}{\pi}\right)^{\frac{1}{3}} \arcsin\left(\frac{\left(\frac{\pi}{6}\right)^{\frac{1}{3}} \omega}{2cN^{\frac{1}{3}}}\right) \frac{1}{c} \frac{1}{\cos\left(arcsin\left(\frac{\left(\frac{\pi}{6}\right)^{\frac{1}{3}} \omega}{2cN^{\frac{1}{3}}}\right)\right)} d\omega \quad (3)$$

On the other hand, the approach proposed by Monachon *et al.* (14), based on irradiance, which assumes that TBC depends on the phonons available in the metal only with no dependence on the substrate properties. This model was implemented using a Debye model with a Sine-Type dispersion relation ($IM_{SineType}$)

The results obtained are given in Fig. 7, 8 and 9 for silicon, sapphire and diamond respectively. In the case of silicon, the irradiance model is shown to lead to predictions reasonably close to the experimental values for all the metals tested. The DMM implemented using a linear dispersion shows large deviation for metals with MTL smaller than 800 MW/m^{2}K roughly, while reasonably good agreement with experimental data is obtained for MTL-values larger than 800 MW/m^{2}K. The DMM implemented with the Sine-type dispersion is observed to be less accurate than the other models in most cases. The exact same tendency is observed for TBC values measured at metal/sapphire interfaces. In the case of diamond, however, the situation is significantly different. The irradiance model is still observed to fit reasonably well the experimental data, while the DMM implemented using a linear dispersion is found to be much less accurate with a precision being lower than a factor of two in all cases. As for silicon and sapphire, the DMM implemented using a Sine-type dispersion is the least accurate model.

These trends are quantified by calculating the average of the logarithm of the ratio of the experimental values found for all metals on a given substrate as compared to the values predicted by one of the tested model. Taking the average of the logarithm of the ($TBC_{\mathrm{exp}}/TBC_{\mathrm{model}}$)-ratios avoids any bias in favour of overestimated values. Averaging over the absolute values of the logarithm of these ratios avoids compensation of positive and negative values. The closer this average is to 0, the more predictive is the model, while taking the standard deviation of all those logs gives the accuracy of the prediction.

$$model\ prediction\ capability = \overline{\left|\log\frac{TBC_{exp}}{TBC_{th}}\right|} \quad (4)$$

$$model\ accuracy = stdev\ \overline{\left|\log\frac{TBC_{exp}}{TBC_{th}}\right|} \quad (5)$$

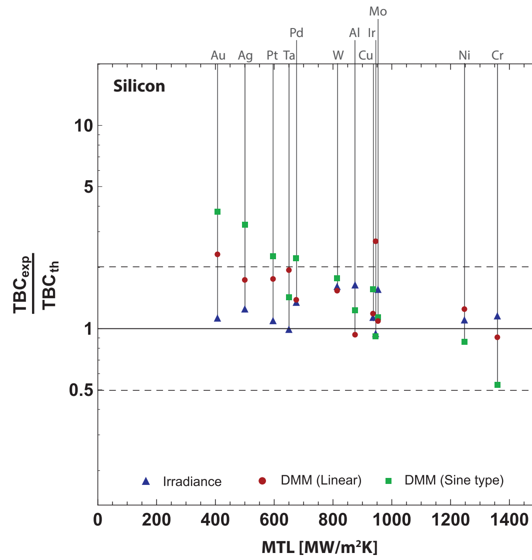

Figure 7: Experimental TBCs for metal/silicon couples compared to predictions obtained using the $IM_{SineType}$, the DMM_{Linear} and the $DMM_{SineType}$.

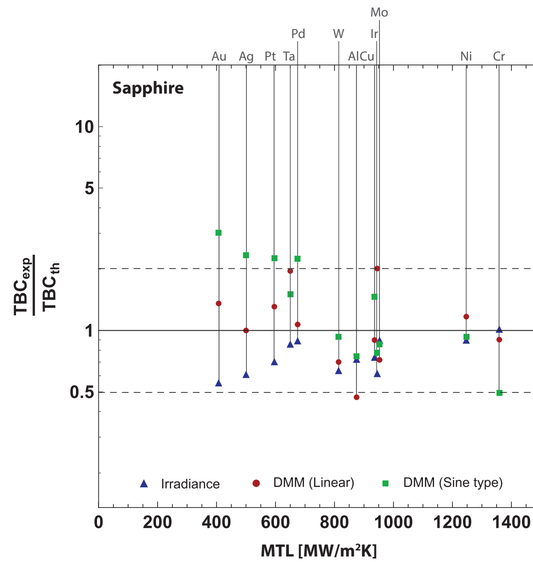

Figure 8: Experimental TBCs for metal/sapphire couples compared to predictions obtained using the $IM_{SineType}$, the DMM_{Linear} and the $DMM_{SineType}$.

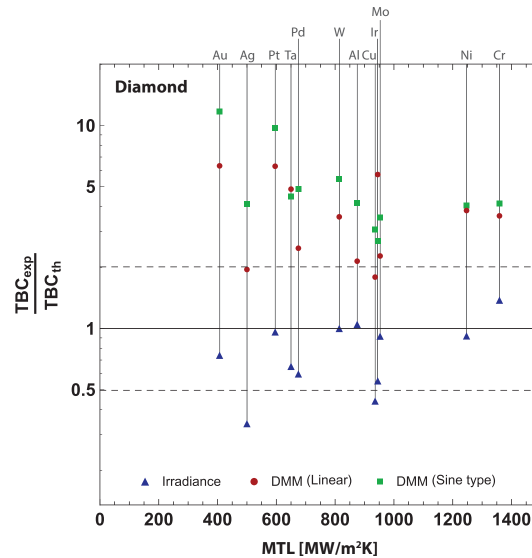

Figure 9: Experimental TBCs for metal/diamond couples compared to predictions obtained using the $IM_{SineType}$, the DMM_{Linear} and the $DMM_{SineType}$. Data for Al, Cr, Mo, Pt and W were taken from Ref (15).

As shown in Fig. 10 and as expected from the above discussion, the $IM_{SineType}$ and the DMM_{Linear} are in average equally precise in predicting TBC at metal/silicon and metal/sapphire interfaces, while the $IM_{SineType}$ is clearly the most suitable model to predict TBC at metal/diamond interfaces. The average precision of the model(s) that is (are) the most accurate to predict the TBC values obtained for each substrate is observed to be roughly constant, i.e around ±35%.

Based on these observations, the following general tendencies can be drawn. The models currently available to predict the TBC reach an average precision of ±35% at best. If DMM_{Linear} seems to be a good option in predicting TBC at metal/silicon and metal/sapphire interfaces, $IM_{SineType}$ is observed to be the most appropriate choice if no restriction is set to the substrate since it keeps its predictive capacity also for metal/diamond. This suggests that substrate influence if not being zero is at least much weaker than predicted by the DMM.

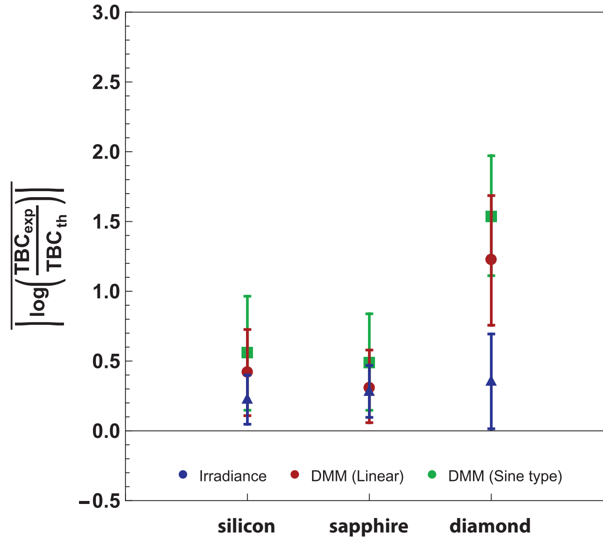

Figure 10: Comparison of the average precision and its standard deviation of each model as compared to experimental data using silicon, sapphire and diamond substrates.

V. CONCLUSION

The effect of surface termination (HF-dipped or RF-etched) on TBC at metal/Si interfaces was studied for a large variety of metal/Si couples. An exploration of the detailed structure of these interfaces allowed identifying two different scenarios: i) Some intermixing exists for both the HF-dipped and the RF-etched samples, which results in TBC values that are independent on surface termination. This suggests that interfacial bonding is the key parameter controlling the TBC at these interfaces, while the intermixed region composition and/or thickness has only little influence; ii) Chemically abrupt interfaces are obtained, resulting in strong differences between the metal/HF-dipped Si and the metal/RF-etched Si interfaces structure. The former is flat, while the latter contains some amount of disordered silicon, which results in TBC values that are always lower for RF-etched samples. This suggests that disordered silicon strongly scatters phonons, resulting in a reduced phonon transmission probability.

The effect of the substrate on TBC was further evaluated by comparing the results obtained at metal/silicon, metal/sapphire and metal/diamond interfaces. A comparison of the experimental data to the DMM and to an approach based on

the metal irradiance allowed concluding that the DMM_{linear} allows predicting TBC with a precision that is similar to the $IM_{SineType}$ for both metal/silicon and metal/sapphire interfaces. The $IM_{SineType}$ is however significantly more accurate at metal/diamond interfaces. The $DMM_{SineType}$ has the poorest precision in all cases. These results suggest that the TBC dependence on substrate is much weaker than predicted by the DMM. Therefore, the $IM_{SineType}$ appears to be the safest choice when trying to predict TBC with an average precision that reaches ±35%.

ACKNOWLEDGEMENTS

The authors are grateful to the SNSF (Project No 200021_149290) for its financial support. Prof. O. Martin from the Nanophotonics and Metrology Laboratory (NAM, EPFL) is warmly thanked for providing the laser source. Dr. A. Magrez from the iPhys platform (EPFL) is acknowledged for his support with the Empyrean diffractometer and Dr. C. Monachon is acknowledged for having provided the code that enables TDTR data analysis

BIBLIOGRPAHY

1. Lyeo, H. K., & Cahill, D. G., Thermal conductance of interfaces between highly dissimilar materials. *Physical Review B*, 73(14) (2006) 144301, DOI: 10.1103/PhysRevB.73.144301

2. Stoner, R. J., & Maris, H. J., Kapitza conductance and heat flow between solids at temperatures from 50 to 300 K. *Physical Review B*, 48(22) (1993) 16373, DOI: 10.1103/PhysRevB.48.16373

3. Losego, M. D., Grady, M. E., Sottos, N.R., Cahill, D. G., & Braun, P. V., Effects of chemical bonding on heat transport across interfaces. *Nature materials*, 11(6) (2012) 502, DOI: 10.1038/nmat3303

4. Monachon, C., & Weber, L., Influence of diamond surface termination on thermal boundary conductance between Al and diamond. *Journal of Applied Physics*, 113(18) (2013) 183504, DOI: 10.1063/1.4804061

5. Collins, K. C., Chen, S., & Chen, G., Effects of surface chemistry on thermal conductance at aluminum–diamond interfaces. *Applied Physics Letters*, 97(8) (2010) 083102, DOI: 10.1063/1.3480413

6. Hopkins, P. E., Phinney, L. M., Serrano, J. R., & Beechem, T. E., Effects of surface roughness and oxide layer on the thermal boundary conductance at aluminum/silicon interfaces. *Physical Review B*, 82 (2010) 085307, DOI: 10.1103/PhysRevB.82.085307

7. Duda, J. C., & Hopkins, P. E., Systematically controlling Kapitza conductance via chemical etching. *Applied Physics Letters*, 100(11) (2012) 111602, DOI: 10.1063/1.3695058

8. Ih Choi, W., Kim, K., & Narumanchi, S., Thermal conductance at atomically clean and disordered silicon/aluminum interfaces: A molecular dynamics simulation study. *Journal of Applied Physics*, 112(5) (2012) 054305, DOI: 10.1063/1.4748872

9. Hopkins, P. E., Duda, J. C., Petz, C. W., & Floro, J. A., Controlling thermal conductance through quantum dot roughening at interfaces. *Physical Review B*, 84(3) (2011) 035438, DOI: 10.1103/PhysRevB.84.035438

10. Swartz, E. T., Solid-solid Thermal Boundary Resistance (1987)

11. Reddy, P., Castelino, K., & Majumdar, A., Diffuse mismatch model of thermal boundary conductance using exact phonon dispersion. *Applied Physics Letters*, 87(21) (2005) 211908. DOI: 10.1063/1.2133890

12. Beechem, T., Graham, S., Hopkins, P., & Norris, P., Role of interface disorder on thermal boundary conductance using a virtual crystal approach. *Applied Physics Letters*, 90(5) (2005) 054104, DOI: 10.1063/1.2437685

13. Hopkins, P. E., Multiple phonon processes contributing to inelastic scattering during thermal boundary conductance at solid interfaces. *Journal of Applied Physics*, 106(1) (2009) 013528, DOI: 10.1063/1.3169515

14. Monachon, C., Weber, L., & Dames, C., Thermal boundary conductance: A materials science perspective. *Annual Review of Materials Research*, 46 (2016) 433, DOI: 10.1146/annurev-matsci-070115-031719

15. Monachon, C., Thermal boundary conductance between metals and dielectrics, (2013) DOI: 10.5075/epfl-thesis-5872

16. Hull, R. (Ed.)., Properties of crystalline silicon (No. 20). IET, (1999).

17. Björck, M., & Andersson, G., GenX: an extensible X-ray reflectivity refinement program utilizing differential evolution. *Journal of Applied Crystallography*, 40(6) (2007) 1174, DOI: 10.1107/S0021889807045086

18. Kang, K., Koh, Y. K., Chiritescu, C., Zheng, X., & Cahill, D. G., Two-tint pump-probe measurements using a femtosecond laser oscillator and sharp-edged optical filters. *Review of Scientific Instruments*, 79(11) (2008) 114901, DOI: 10.1063/1.3020759

19. Cahill, D. G., Analysis of heat flow in layered structures for time-domain thermoreflectance. *Review of scientific instruments*, 75(12) (2004) 5119, DOI: 10.1063/1.1819431

20. Haynes, W. M. (Ed.), CRC handbook of chemistry and physics. CRC press, (2014).

21. Minnich A.J., Johnson J.A., Schmidt, A.J., Esfarjani K., Dresselhaud M.S., Nelson K.A., Chen G., Thermal Conductivity Spectroscopy Technique to Measure Phonon Mean Free Paths, *Physic Review Letters*, 107 (2011) 95901, DOI: 10.1103/PhysRevLett.107.095901

22. Oh, D. W., Kim, S., Rogers, J. A., Cahill, D. G., & Sinha, S., Interfacial Thermal Conductance of Transfer-Printed Metal Films. *Advanced Materials*, 23(43) (2011) 5028, DOI: 10.1002/adma.201102994

23. Jeong, M., Freedman, J. P., Liang, H. J., Chow, C.-M., Sokalski, V. M., Bain, J. A., & Malen, J. A., Enhancement of thermal conductance at metal-dielectric interfaces using subnanometer metal adhesion layers. *Physical Review Applied*, 5(1) (2016) 014009, DOI: 10.1103/PhysRevApplied.5.014009

24. Freedman, J. P., Yu, X., Davis, R. F., Gellman, & A. J., Malen, J. A., Thermal interface conductance across metal alloy–dielectric interfaces. *Physical Review B*, 93(3) (2016) 035309, DOI: 10.1103/PhysRevB.93.035309

25. Hopkins, P. E., Salaway, R. N., Stevens, R. J., & Norris, P. M., Temperature-Dependent Thermal Boundary Conductance at Al/Al_2O_3 ant Pt/Al_2O_3 interfaces, International Journal of Thermophysics, 28 (2007) 947, DOI: 10.1007/s10765-007-0236-5

26. Hohensee G., Wilson R.B., & Cahill D.G., Thermal conductance of metal–diamond interfaces at high pressure, *Nature Communications*, 6 (2015) 6578, DOI: 10.1038/ncomms7578

27. Klement, W., Metastable close packed structures in Silver-rich Binary alloys with tin, antimony, and silicon, *Trans. Met. Soc*. AIME 233 (1965) 1182

28. Jun, W. K., Willens, R. H., & Duwez, P. O. L., Non-crystalline structure in solidified gold–silicon alloys. *Nature*, 187(4740) (1960) 869, DOI: 10.1038/187869b0

29. Hamaoui G., Horny N., Hua Z., Zhu T., Robillard J-F., Fleming A., Ban H., Chirtoc M., Electronic contribution in heat transfer at metal-semiconductor and metal silicide-semiconductor interfaces, *Scientific Reports*, 8 (2018) 11352, DOI: 10.1038/s41598-018-29505-4.

30. Ye N., Feser J.P., et al., Sadasivam S., Fisher T. S., Wang T., Ni C., Janotti A., Themal transport across metal silicide-silicon interfaces: An experimental comparison between epitaxial and nonepitaxial interfaces, *Physical Review B*, 95 (2017) 85430, DOI: 10.1103/PhysRevB.95.085430

31. Neshpor V.S., The thermal conductivity of the silicides of transition metals, *Journal of engineering physics*, 15 (1968) 750, DOI: 10.1007/BF00829703

32. Monachon C., & Weber, L., Thermal boundary conductance between refractory metal carbides and diamond, *Acta Mater*, 73 (2014) 337, DOI: 10.1016/j.actamat.2014.04.024

33. Dames C., & Chen G., Theoretical phonon thermal conductivity of Si/Ge superlattice nanowires, Journal of Applied Physics, 95 (2004) 682, DOI: 10.1063/1.1631734